

Dynamic interactions between cohesive sediment tracers and natural mud

Kate L. Spencer · Andrew J. Manning ·
Ian G. Droppo · Gary G. Leppard · Thomas Benson

Received: 22 April 2010 / Accepted: 19 August 2010 / Published online: 1 September 2010
© Springer-Verlag 2010

Abstract

Purpose Cohesive sediment tracers have been developed to improve our understanding of fine sediment transport in the aquatic environment. However, there is little understanding of their physical and dynamic characteristics compared to the natural sediments they are intended to mimic. This work focuses on a labelled clay mineral tracer examining its dynamic characteristics and determining whether it flocculates and interacts with natural estuarine mud.

Materials and methods Gross floc characteristics (size and settling velocity) were measured using video image analysis. Floc density, porosity and mass settling flux were then calculated. Fine-scale floc internal structure and composition were observed using transmission electron microscopy (TEM). The interaction of the tracer and natural

mud was examined by observing tracer and natural mud mixtures.

Results and discussion The tracer formed macroflocs ($>160\ \mu\text{m}$) that could not be distinguished statistically from natural mud, whilst tracer microflocs ($<160\ \mu\text{m}$) were smaller and settled more slowly. Gross settling characteristics and TEM analysis indicate that the tracer and natural mud do not interact on a primary particle-to-particle basis, although microflocs of pure tracer and mud do interact. The physical and dynamic floc properties of tracer and natural mud mixtures were different from both pure tracer and pure natural mud due to the irregular packing of differently shaped natural mud and tracer flocs.

Conclusions The cohesive tracer flocculates and has similar physical and dynamic properties to natural mud; however, when the tracer interacts with natural mud, it forms flocs with significantly different characteristics. These mixed flocs exhibit different transport characteristics (e.g. settling velocity) to natural muddy material. Therefore, cohesive sediment tracers may not accurately predict cohesive sediment transport pathways, and this has implications for the use of cohesive tracers to understand natural mud transport and to develop sediment transport models.

Responsible editor: Gijs D. Breedveld

K. L. Spencer (✉)
Department of Geography, Queen Mary University of London,
Mile End Road,
London E1 4NS, UK
e-mail: k.spencer@qmul.ac.uk

A. J. Manning
School of Marine Science and Engineering,
University of Plymouth,
Portland Square, Drake Circus,
Plymouth, Devon PL4 8AA, UK

I. G. Droppo · G. G. Leppard
Environment Canada,
867 Lakeshore Rd.,
Burlington, ON, Canada

T. Benson
HR Wallingford Ltd.,
Howbery Park,
Wallingford, Oxfordshire OX10 8BA, UK

Keywords Cohesive sediment · Floc structure · Sediment tracer · Sediment transport

1 Introduction

Understanding the dispersion patterns of the fine sediment fraction ($<63\ \mu\text{m}$) is fundamental to the sustainable management of freshwater, estuarine and fully marine environments. Prediction of sediment movement and dispersion requires accurate and reliable field techniques

for the measurement of sediment transport pathways and the subsequent development and validation of sediment transport models.

Protocols for the measurement of transport pathways of sand-sized sediment ($>63\ \mu\text{m}$) in the field are very well established using either sediment trend analysis (STA) or sediment tracing techniques. STA relies on the assumption that grain size characteristics, such as size, sorting and skew, are dependent on sediment transport processes (McLaren and Bowles 1985; Le Roux and Rojas 2007; McLaren et al. 2007) and trends in these characteristics indicate different transport scenarios. However, as fine sediment is transported, it undergoes flocculation with physical and transport characteristics of individual particles continually changing. Consequently, it is difficult to extract meaningful information on transport pathways using STA for fine-grained, cohesive sediment (Poizot et al. 2008).

Black et al. (2007) have recently reviewed the use of sediment tracers for measuring sediment transport pathways and they identify two basic tracer particle types: natural particles that have been labelled with a measurable and identifiable “signature” and synthetic particles. Such signatures include radioactivity and fluorescent dyes, and although radioactive tracers have been successful (Courtois and Monaco 1969; Heathershaw and Carr 1978), there is little scope for their further use due to current environmental concerns and cost. The use of fluorescent dyes has been widely used to examine sediment transport dynamics in a range of coastal settings (e.g. Silva et al. 2007; Tonk and Masselink 2007). However, their use is restricted to the $>63\ \mu\text{m}$ fraction as coating natural silts and clays significantly modifies particle size and density, and hence transport characteristics (Black et al. 2007). As flocculation is in part a result of surface charges, coating particles may also alter this important natural process, significantly altering the particle’s transport behaviour (Droppo 2004).

Consequently, there has been considerable effort within the scientific community to develop a tracer for the fine sediment fraction including the use of synthetic tracer particles and the labelling of natural clays. The commercial sector has developed synthetic, polymer-based fluorescent tracers with the same size, density and surface charge characteristics as the flocculated clay and silt fraction. For example, fluorescent paint pigments have been used to track the dispersion of contaminated sediments from combined sewer outfalls (e.g. Adams 1998). Natural clays have been labelled with DNA (Mahler et al. 1998a), iridium (Yin et al. 1993) and rare earth elements (REEs; Krezoski 1985; Mahler et al. 1998b; Spencer et al. 2007) and used to measure fine sediment transport pathways in a number of aquatic environments including estuaries, lakes, groundwater, shallow seas and karst systems. However, none of these

techniques have been widely used by the regulatory authorities for the management of fine sediment for a number of reasons. Firstly, although there have been a small number of geochemical tracer release experiments, these have been carried out with relatively little prior understanding of the tracer’s physical behaviour, particularly in saline environments. Secondly, where tracer studies have been carried out, it is often under contract and results are not published. Consequently, little material is available in the public domain for scientific scrutiny and few data are available on which to base a precedent for a methodological framework.

An overarching assumption of tracer technology is that the tracer sediment has the same physical and transport properties as the natural sediment that it is intended to mimic. For non-cohesive sand-sized materials, matching particle size, shape, density and transport characteristics is achievable. However, as cohesive sediment is transported primarily as flocs (Droppo 2001), it is critical that any cohesive sediment tracer must flocculate (on its own or in conjunction with the natural sediment of study) and must have similar dynamic characteristics to natural flocculated material (i.e. erosion, transport and settling). This must be demonstrated before the use of synthetic particles or naturally labelled clays can be validated and accepted by the user community as tracers. Synthetic tracers have been generated with similar size distributions to the cohesive sediment fraction, but these materials are spherical in shape, with high hydrophobicity, meaning that their flocculation characteristics and interaction with other natural particles in suspension vary considerably from their natural clay and silt counterparts (Newmann et al. 1990). Therefore, the use of synthetic particles may not satisfy the basic assumptions of tracer technology. There are few studies examining the physical behaviour of naturally labelled clay tracers, and most studies are limited to the examination of gross settling characteristics (Louisse et al. 1986) rather than flocculation behaviour and its impact on sediment transport.

Here, we have examined the physical characteristics of a cohesive sediment tracer and its interaction with natural estuarine mud in saline environments. The sediment tracer used was a holmium (Ho)-labelled montmorillonite, which has recently been proposed as a potential cohesive sediment tracer (Spencer et al. 2007). The objectives of this work were to examine the physical characteristics, internal structure and settling dynamics of flocculated tracer sediment compared to natural mud and to determine whether the tracer sediment interacted with natural estuarine muds under laboratory conditions at both fine and gross scales, defined for the purpose of this paper by the resolution of the analytical/observational techniques used. To our knowledge, this is the first study examining the flocculation characteristics and structure of cohesive

sediment tracers and their interaction with natural sediment and consequently provides protocols that can be applied to the investigation of other cohesive tracers in a range of aquatic environments.

2 Methodology

2.1 Materials

The tracer sediment used was a Ho-labelled montmorillonite clay. Montmorillonite, a 2:1 aluminosilicate commonly found in estuarine sediments, was labelled with Ho, one of the rare earth elements. Holmium is present at low geochemical background concentrations, can be easily incorporated into the clay mineral lattice, can be measured routinely using ICP analytical techniques and is a useful geochemical “signature” to measure. Montmorillonite was labelled with Ho in batch sorption experiments. The conditions for sorption were as follows: clay mineral/Ho solution ratio (1:10), Ho solution concentration (0.025 M), ionic strength (NaNO_3 , 0.01 M), pH 5, temperature (20°C) and equilibration time (72 h). Details for its preparation, preliminary field trials, chemical behaviour and toxicity in the environment are presented elsewhere (Grapentine et al. 2007; Spencer et al. 2007). The labelled clay has a Ho content of approximately 40,000 mg kg⁻¹ and following preparation was dried and ground to <63 µm using a Tema ball mill. Herein, the Ho-labelled montmorillonite clay will be called the “tracer”.

The natural estuarine muds used in these experiments were collected from the Calstock region of the Tamar Estuary in SW England. These muds have been very well characterised in terms of their physical flocculation behaviour (settling velocity, size distributions, effective density and floc mass; Dyer et al. 2002; Manning and Dyer 2002, 2007). Herein, these sediments will be called “natural mud”.

2.2 Gross-scale analysis

A series of “jar tests” (see <http://www.phippsbird.com/jar.html> and Environmental Protection Agency 1999) were conducted in order to assess how the tracer behaved in a turbulent water when combined with natural mud. A sediment slurry at a predetermined concentration was placed in a glass jar and then the suspension was agitated using a stirring bar (suspended in the fluid) for a duration sufficiently long enough for the flocs formed to reach a quasi-equilibrium state of flocculation. This technique is often used as a first line in assessing and comparing the physicochemical interactions of substances such as flocculated natural mud suspensions (e.g. Bouyer et al. 2005; Mietta et al. 2009), and in this instance the tracer.

A comprehensive series of floc characteristics tests were conducted for the tracer using tracer-to-natural mud ratios (T/M) of 0 T:100 M (i.e. pure natural mud), 25 T:75 M, 50 T:50 M, 75 T:25 M and 100 T:0 M (i.e. pure tracer) all at a suspended particulate matter (SPM) concentration of 1 g L⁻¹. This SPM concentration was chosen as it is high enough to enable flocs to form easily and yet is environmentally realistic of highly turbid, estuarine bottom waters. A high concentration slurry of Tamar mud was initially mixed in a 10-L basin, and whilst continually being kept in suspension, the average concentration of this “base stock” was determined by gravimetric analysis. The required volume of the base stock to produce the desired target suspended concentration and tracer-to-natural mud ratio was decanted into a 1-L graduated glass beaker. The remaining tracer was added to the muddy suspension as a dry weight and both mixed together with 1 L water (salinity 30 ± 0.5 psu). Each suspension was stirred for approximately 30 min to allow the particles sufficient time to flocculate and attain floc equilibrium in accordance with the theoretical flocculation time (van Leussen 1994). The level of turbulent shear stress within the jar was approximately 0.3–0.4 Pa (calibration protocols are outlined by Hudson 1981 and Droste 1996), providing the ideal stimulation for maximum floc growth (Manning 2004a).

Floc size, represented as spherical equivalent diameter (D) and settling velocity (W_s) were obtained using the Laboratory Spectral Flocculation Characteristics instrument (LabSFLOC, Manning 2006). LabSFLOC is a low intrusive floc sampling device which uses a high-resolution monochromatic video camera to measure simultaneously the floc sizes and settling velocities of a floc population as it settles in still water. The lower resolution of the LabSFLOC instrument is approximately 20 µm, and this defines the lower limit of our gross-scale investigations.

Following turbulent agitation, a floc suspension was carefully extracted from the main suspension using an inverted modified pipette (Manning et al. 2007). The captured flocs were then allowed to pass from the pipette into the LabSFLOC settling column (without any mechanical assistance) and undergo natural gravitational settling through the water column. The video camera was positioned in the side wall of the settling column 75 mm above the base, viewing all flocs in the centre of the column that passed within a 1-mm depth of field, 45 mm from the high-magnification video camera lens. The LabSFLOC column water had the same salinity as that used for the jar tests.

Recorded video images of the settling flocs were then used to derive measurements of floc D and W_s . The simultaneous direct measurements of D and W_s meant that the effective density (ρ_e , density of the floc minus density of the water) could be calculated via Stokes’ law. If a floc demonstrated a particle Reynolds number > 0.5, the Oseen

modification was applied in order to correct for the increased inertia during settling (ten Brinke 1993). Other parameters including floc porosity (P), floc dry mass and the mass settling flux (MSF) were also calculated using algorithms developed by Fennessy et al. (1994) and modified by Manning (2004b).

2.3 Fine-scale analysis

The internal fine-scale structure of flocs was assessed using transmission electron microscopy (TEM, 1- to 3-nm practical resolution at highest magnification) and energy-dispersive spectroscopy (EDS; Buffle and Leppard 1995). Floc samples were prepared by first generating a sediment suspension in artificial seawater solution. For all experiments, a 34 g L⁻¹ seawater solution was made up using Sigma[®] sea salts. The sediments used comprised tracer-to-natural mud ratios (T/M) of 0 T:100 M, 50 T:50 M and 100 T:0 M. A 50:50 tracer-to-natural mud mix was achieved by thoroughly mixing dried, ground tracer and wet natural mud in a Barnant[®] mixer with enough artificial seawater to form a fluid slurry. The sediments were then added to artificial seawater at a SPM concentration of 1 g L⁻¹ to match the gross-scale experiments. To encourage flocculation, the suspension was stirred very gently using a magnetic stirrer, providing just enough motion to suspend the sediments without creating turbulence that might destroy subsequent flocs. Suspensions of the three flocculated sediments (0 T:100 M, 50 T:50 M and 100 T:0 M) were then transferred to 50-mL polypropylene vials using a pipette and stored at 4°C until TEM and EDS analyses were performed within 24 h.

Samples were prepared for TEM analysis following the protocols of Liss et al. (1996) by first stabilising the samples in buffered glutaraldehyde, immersing in buffered osmium tetroxide and then embedding the samples in Spurr low-viscosity epoxy resin. Small volumes of the suspended sediment flocs were added to 15-mL screw top vials containing 3% glutaraldehyde and 0.1% ruthenium red (buffered with 0.1 M Na-cacodylate at pH 7.1). The samples were stored in a refrigerator overnight, followed by centrifugation at 300× g for 10 min, and then washed (to remove excess glutaraldehyde) three times in 0.1 M Na-cacodylate buffer (pH 7.1). This was followed by a resuspension (secondary fixation) in a mixture of osmium tetroxide (1%) and ruthenium red (0.05%). Ultrathin sections of the polymerised resins (80- to 100-nm thickness) were obtained by sectioning with a diamond knife mounted in an ultramicrotome (LEICA Ultra-cut UCT, LEICA Microsystems, Wien, Austria). The ultrathin sections were mounted on Formvar-covered copper grids for morphological analysis; for EDS, the sections were also carbon-coated. The field of view for these images is

typically ≤ 20 μm , and this defines the resolution of our fine-scale analyses.

The ultrathin sections were then observed in transmission mode (TEM) at an accelerating voltage of 80 kV using a JEM 1200 EX TEMSCAN scanning transmission electron microscope (STEM; JEOL, Peabody, MA, USA). The scanning mode of the STEM was used to generate a microprobe beam for EDS of individual floc components in sections, allowing the observation of the distribution of Ho-labelled components within the flocs. A Tracor Northern X-ray detector (Noran, Madison, WI, USA) with EDS 2004 microanalysis software (IXRF Systems, Inc., Houston, TX, USA) provided energy-dispersive X-ray spectra (on a structure-selective basis) of all elements $Z > 10$.

3 Results

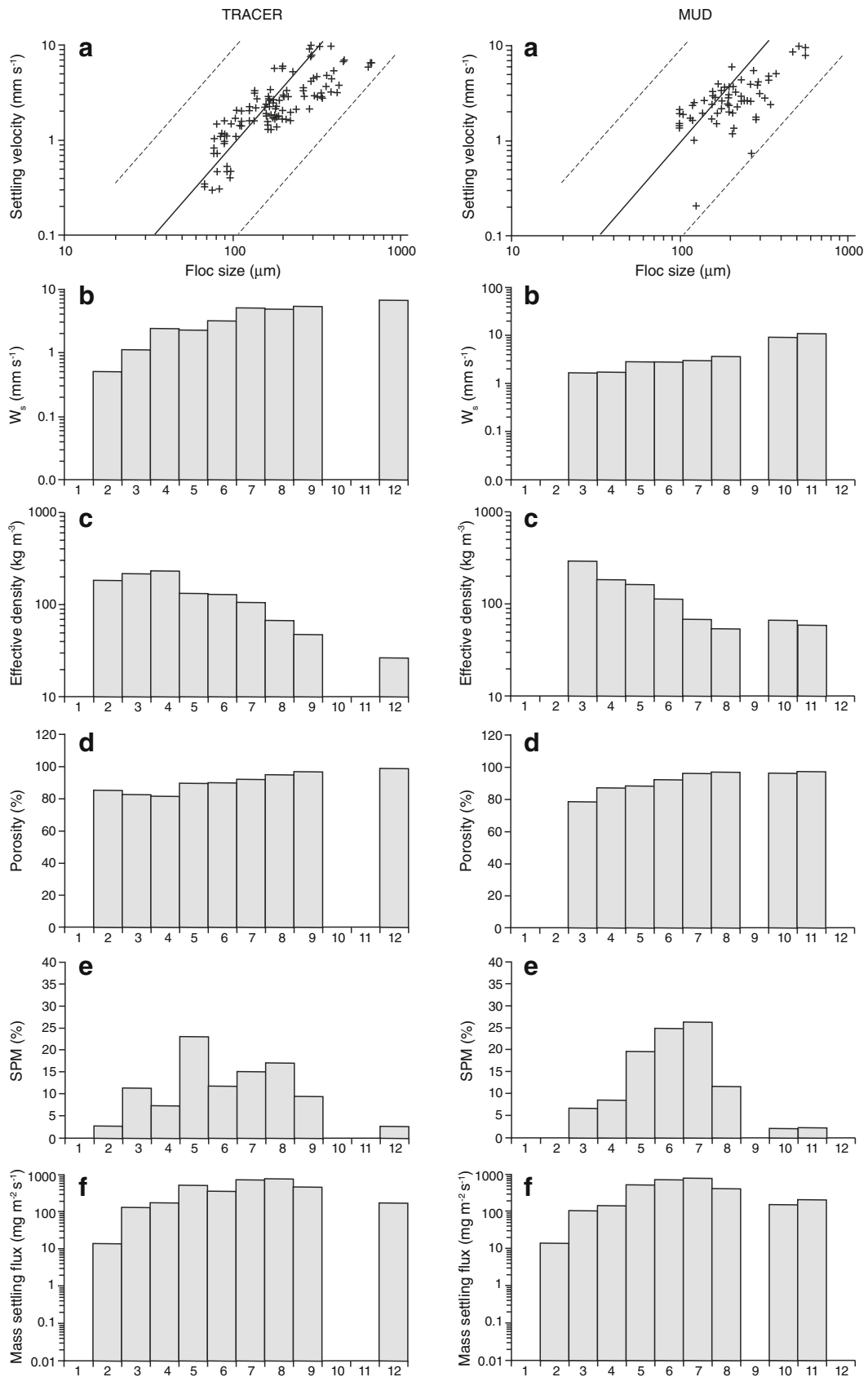
3.1 Gross-scale analysis

The tracer and natural mud samples were initially compared in terms of the measured characteristics of the total floc populations. Scatter plots of floc size plotted against W_s are given for the tracer and natural mud (Fig. 1a). The tracer flocs ranged from 53 to 680 μm (size band (SB) 2–12) in diameter, whilst individual floc W_s ranged from 0.2 to 10 mm s^{-1} . The individual natural mud flocs ranged in size from 97 to 588 μm (SBs 3–11), whilst W_s ranged from 0.2 to 11.2 mm s^{-1} . Mean values for D and W_s are given in Table 1. The diameter and settling velocities of the tracer and natural mud floc populations are within similar ranges. However, the floc populations are statistically different, with the tracer having a smaller floc size and slower settling velocity than the natural mud ($U(776)=228,735$, $z=-6.30$, $p<0.001$ and $U(724)=239,818$, $z=-4.98$, $p<0.001$, respectively).

The mean effective density ($\rho_{e \text{ mean}}$) and mean porosity (P_{mean}) for the tracer and natural mud total floc populations were similar with the tracer forming slightly denser, less porous flocs than the natural mud (see Table 1). Structurally, both the tracer and natural floc populations exhibited similar trends with P increasing and ρ_e decreasing as the flocs increase in size (see Fig. 1c, d). The ρ_e for the tracer population ranged from 26 kg m^{-3} ($P=98\%$) to 418 kg m^{-3} ($P=67\%$), whilst the natural mud flocs ranged from 17 kg m^{-3} ($P=99\%$) to 366 kg m^{-3} ($P=71\%$).

There may be considerable variability in the physical and dynamic characteristics of flocs across an entire floc population. Therefore, it is often appropriate to divide the floc population into subcomponents or to examine charac-

Fig. 1 Floc property distributions: **a** settling velocity vs diameter, **b** settling velocity, **c** effective density, **d** porosity, **e** SPM% and **f** MSF for tracer and natural mud



Size band	1	2	3	4	5	6	7	8	9	10	11	12
Size μm	20–40	40–80	80–120	120–160	160–200	200–240	240–320	320–400	400–480	480–560	560–640	>640

Table 1 Mean values for total floc population characteristics

LabSFLOC sample	Total mass settling flux ($\text{mgm}^{-2}\text{s}^{-1}$)	Floc size (mm)	Effective density (kgm^{-3})	Settling velocity (mms^{-1})	Fractal dimension (nf)	H/W ratio	Porosity (%)
100%T	3,317	192.39	151.18	2.57	2.42	1.36	87.96
25%T	3,704	321.24	100.94	3.34	2.35	1.23	91.96
50%T	3,447	291.69	77.51	2.75	2.29	1.42	93.83
75%T	3,305	224.72	154.33	2.94	2.41	1.33	87.71
MUD	2,981	208.21	140.82	2.65	2.42	2.27	88.79

teristics over the floc size spectrum. Commonly used subcomponents are microflocs ($D < 160 \mu\text{m}$) and macroflocs ($D > 160 \mu\text{m}$; Manning 2001). Microflocs have the highest particle concentration in estuarine environments and are considered to be the building blocks for larger aggregates. Macroflocs are present in lower numbers but have fast settling velocities and are responsible for the majority of the mass settling load, particularly in the estuarine turbidity zone (Benson and French 2007; Dyer et al. 2002; Eisma 1986). Therefore, measuring the characteristics of macrofloc populations is fundamental to understanding fine sediment transport dynamics. Figure 1 shows the average physical and dynamic floc characteristics as distributed over the floc size spectrum, whilst Tables 2 and 3 present the mean floc characteristics for microflocs and macroflocs, respectively.

Mean values for D , ρ_e , W_s and P for the tracer and natural mud microfloc population are within similar ranges (see Table 2). However, a Mann–Whitney test (SPSS 16.0) demonstrated that the tracer forms significantly smaller and slower settling microflocs than the natural mud ($U(481)=16,503$, $z=-7.38$, $p<0.001$). For the tracer microfloc population, ρ_e ranged from 182 to 231 kg m^{-3} and porosity ranged from 81% to 85%, whilst the natural mud microflocs had ρ_e ranging from 179 to 283 kg m^{-3} and P ranging from 77% to 86%. The mean physical and dynamic characteristics of the tracer and natural mud macrofloc populations are similar and cannot be distinguished statistically (Table 3).

The two-dimensional shape of the flocs was also observed and described according to height-to-width ratios (H/W). The tracer and natural mud flocs have distinctly different shapes with the tracer having a sub-spheroidal shape, whilst the natural mud is forming more elongate “stringer” type flocs ($H/W>2$). This is most pronounced for the macrofloc populations (Table 3).

Figure 1 shows the distribution of floc characteristics across the entire floc size spectrum for the tracer and the natural mud. In general, W_s and P increase, whilst ρ_e decreases as floc size becomes larger for both the tracer and natural mud flocs. The particle concentration across the floc size spectrum for the tracer and natural mud populations is shown in Fig. 1e. For the tracer, the maximum SPM (23%) resides in SB5 (160–200 μm), whilst for the natural mud, 27% of the SPM is in SB7 (240–320 μm), suggesting that mass is distributed differently between the two floc populations.

MSF is defined as the product of the W_s and the SPM concentration. For the tracer, 9% of the total MSF is within the microfloc fraction compared to 8% for the natural mud. However, in terms of total MSF, the tracer produces 3.3 $\text{g m}^2 \text{s}^{-1}$ compared with 3.0 $\text{g m}^2 \text{s}^{-1}$ for the natural mud, indicating that the overall settling dynamics of these two sediments are slightly different.

In order to examine the interaction between the tracer and natural mud, the physical properties of T/M mixtures were also examined and are shown in Figs. 2 and 3 for the microflocs and macroflocs, respectively. A Kruskal–

Table 2 Mean values for microfloc population characteristics

LabSFLOC sample	Total mass settling flux ($\text{mgm}^{-2}\text{s}^{-1}$)	Floc size (mm)	Effective density (kgm^{-3})	Settling velocity (mms^{-1})	Fractal dimension (nf)	H/W ratio (%)	Porosity	SPM%
100%T	310	102.05	213.62	1.32	2.45	1.34	82.99	21.22
25%T	132	112.91	221.20	1.82	2.44	0.98	82.39	6.35
50%T	60	98.59	123.60	0.68	2.22	0.89	90.16	8.16
75%T	228	91.39	331.21	1.83	2.49	1.03	73.63	10.52
MUD	250	118.17	231.20	1.66	2.50	1.76	81.59	14.95

Table 3 Mean values for macrofloc population characteristics

LabSFLOC sample	Total mass settling flux (mgm ⁻² s ⁻¹)	Floc size (mm)	Effective density (kgm ⁻³)	Settling velocity (mms ⁻¹)	Fractal dimension (nf)	H/W ratio (%)	Porosity	SPM%
100%T	3,008	253	109.51	3.40	2.40	1.37	91.28	78.74
25%T	3,572	367	74.43	3.68	2.33	1.29	94.07	93.65
50%T	3,387	352	63.22	3.39	2.32	1.59	94.97	93.85
75%T	3,076	271	92.62	3.33	2.38	1.44	92.63	89.48
MUD	2,731	240	108.49	3.00	2.39	2.44	91.36	85.05

Wallis (SPSS 16.0) test was used to identify significant differences between the measured variables (D and W_s) for the five sediment types, i.e. 0 T:100 M (natural mud), 25 T:75 M, 50 T:50 M, 75 T:25 M and 100 T:0 M (tracer). Where differences were identified, these were explored further using a Mann–Whitney test calculating critical significance values using the Bonferroni procedure (Field 2009).

There are slight differences in the diameter of the T/M microflocs (Fig. 2), although only the 75 T:25 M mixture forms significantly smaller microflocs ($U=21,573$, $Z=-3.55$, $p<0.001$), which also have higher ρ_e . All the microflocs containing any tracer have shapes which are sub-spheroidal to spheroidal with mean H/W ratios between 0.89 and 1.34, whilst the natural mud microflocs are more elongate (H/W=1.76).

There are significant differences between the T/M macrofloc characteristics, with the mixed T/M macroflocs having significantly larger floc diameters and faster settling velocities than both the pure natural mud and tracer macroflocs. The largest macroflocs ($D=367 \mu\text{m}$) were formed from a 25 T:75 M suspension which also had the highest W_s of 3.7 mm s^{-1} . The ρ_e of the macroflocs at each T/M ratio (Fig. 3) were all lower than the pure natural mud and tracer macroflocs, with P ranging from 91% to 95%. This suggests that although the pure natural mud and tracer have similar size and settling characteristics, when the tracer and natural mud are combined, the resultant macroflocs have significantly different structure and behaviour. The percentage of total SPM which comprised the macroflocs varied between 89% and 94% across the T/M mixtures, and this is higher than either the pure natural

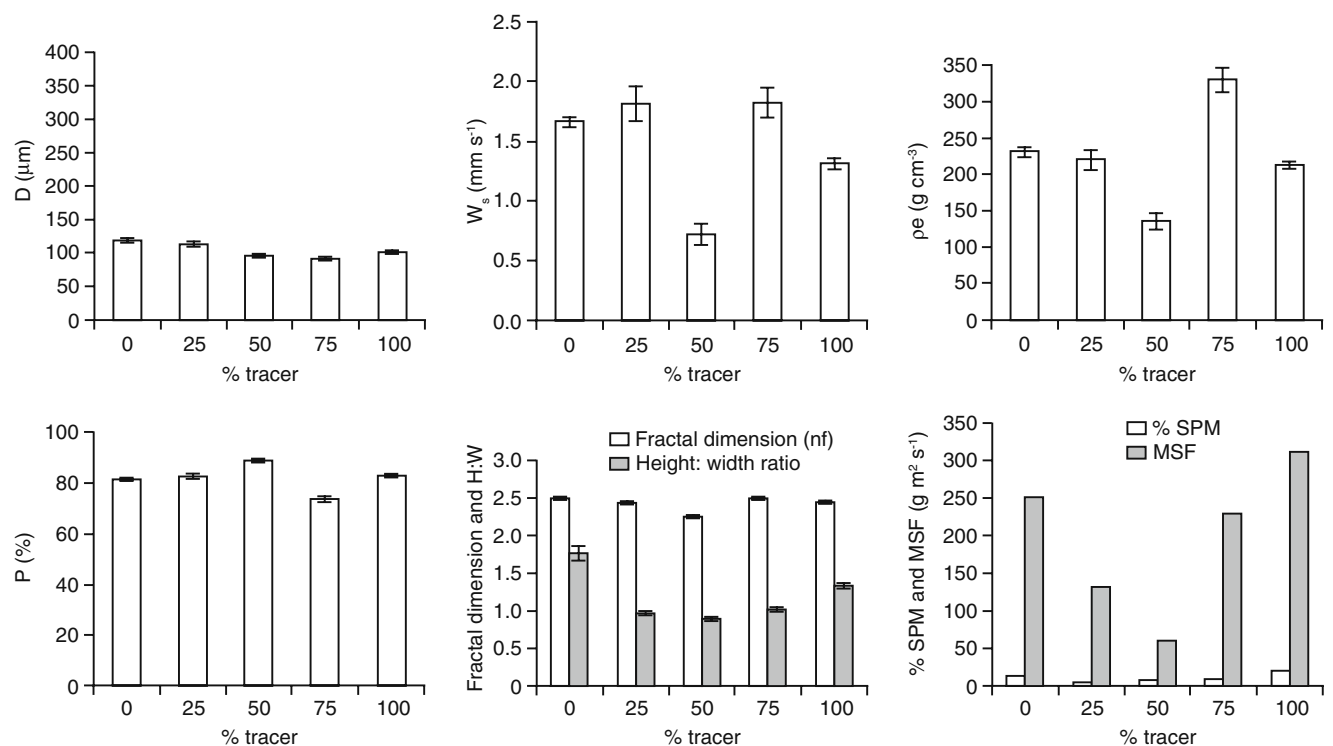


Fig. 2 Average values for microfloc (<160 μm) properties for the T/M mixed flocs with increasing tracer content from 0% to 100%

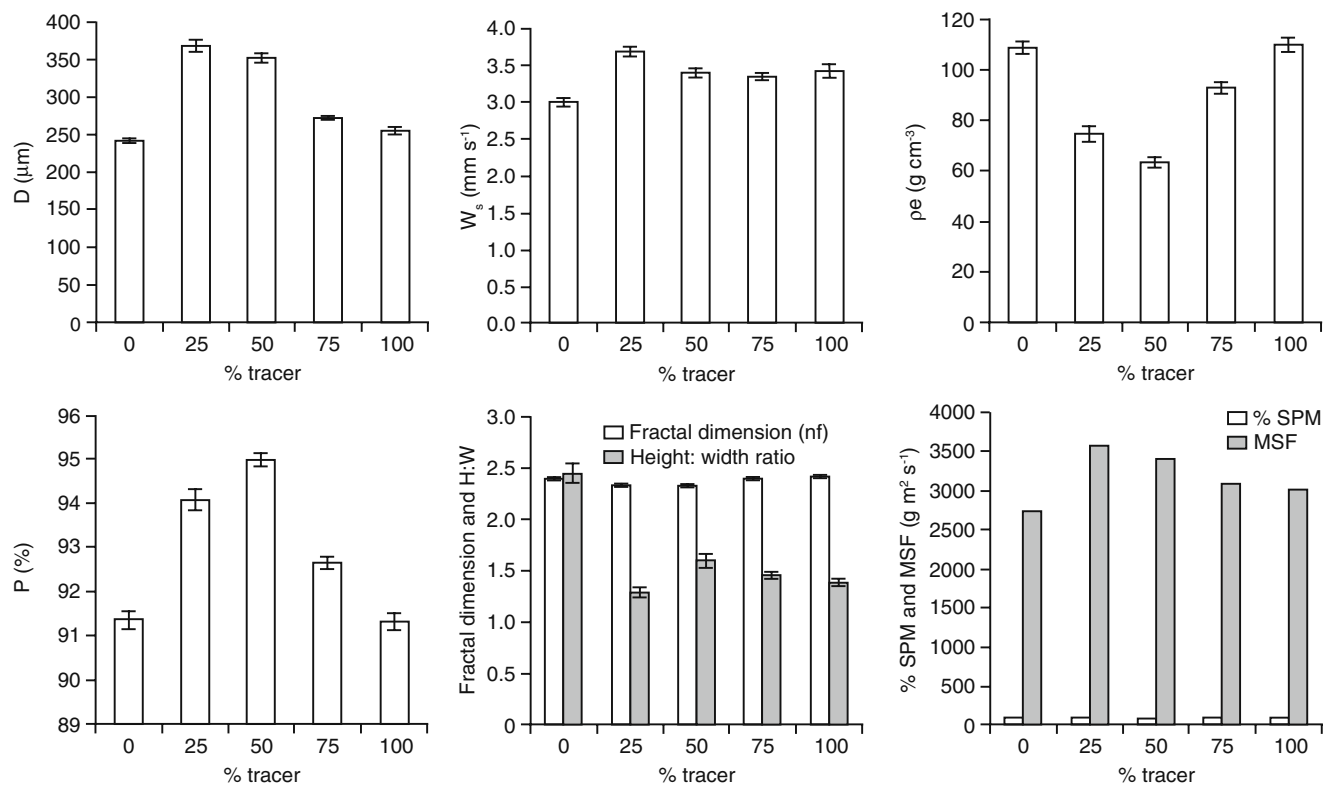


Fig. 3 Average values for macrofloc (>160 μm) properties for the T/M mixed flocs with increasing tracer content from 0% to 100%

mud or the tracer (see Fig. 3). The corresponding MSF of the macrofloc population for the T/M mixtures ranged from 2.7 to 3.5 g m⁻² s⁻¹, with the T/M mixtures all having higher mass settling fluxes than either the pure tracer or the natural mud.

To summarise, the natural mud produced large, low-density, highly porous macroflocs with physical and dynamic characteristics typical of fine, cohesive estuarine sediments. The tracer formed total floc populations with a similar size range to the natural mud, and the tracer and natural mud macrofloc populations could not be distinguished statistically. The tracer formed fewer macroflocs (only 60% were macroflocs compared to 74% of the natural mud population); however, the tracer formed the largest (and smallest) individual flocs. This suggests that flocculation processes and aggregate growth were similar for both the tracer and natural mud. When examining characteristics across the floc size spectrum, SPM and mass settling flux were distributed differently for the tracer and natural mud with a higher MSF for the tracer. The tracer and natural mud form flocs with distinctly different shapes and the presence of any tracer in mixed T/M flocs alters floc shape, resulting on more spheroidal flocs compared with elongate “stringer” natural mud flocs. When the tracer and natural mud interact, they form flocs that are bigger, with faster

settling velocities and lower densities than either pure natural mud or pure tracer.

3.2 Fine-scale analysis

Electron micrographs of natural mud and tracer flocs are shown in Fig. 4. A typical natural mud floc section shows a complex matrix of structurally interdependent components (Fig. 4a). Both organic and inorganic particles are present, creating a highly porous, high water content three-dimensional matrix. The organic constituents are primarily bacteria and their extracellular polymeric substance (EPS) fibrils which are produced by the bacteria for attachment, assimilation of food (dissolved organic carbon) and for protection from predation and contaminants (Gerba and McLeod 1976). The EPS can be seen linking the biological and inorganic particles and represents a microstructural framework of the floc matrix. The EPS matrix is believed to be the component of the floc that enhances floc building and stability (Droppo 2004). The inorganic constituents comprise primarily planar clay minerals, quartz grains (evident from concoidal fracturing), Fe and Mn oxides and opaque, sub-cubic minerals (probably pyrite) typical of estuarine sediments. Whilst bioflocculation is believed to be the most influential floc building process (Droppo

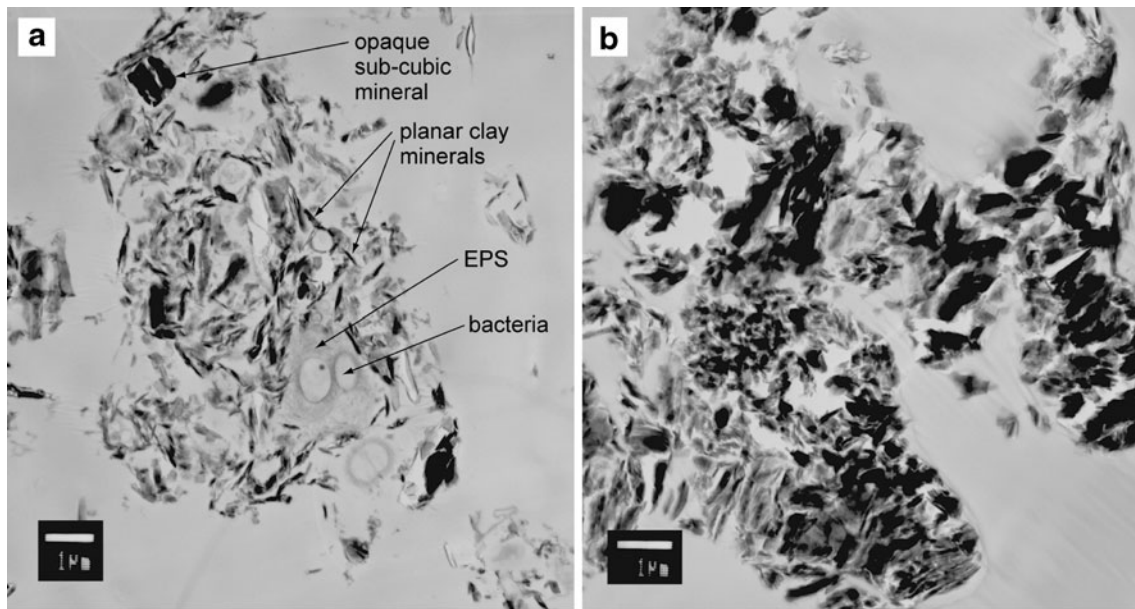


Fig. 4 Electron micrographs of natural mud (a) and tracer flocs (b)

2001), Fig. 4a also demonstrates that electrochemical flocculation has occurred as a number of inorganic particle-to-particle contacts are apparent.

In comparison, the tracer flocs (Fig. 4b) are more dense and inorganic with the montmorillonite platelets clearly present in tight packets. Relative to the natural mud floc, there is reduced pore space and aggregation is clearly controlled by electrochemical flocculation. Figure 5 shows an EDS spectrum typical of the tracer showing peaks for Si, Al, Fe and Ho, although the Ho peak is very small compared to the major elements. Ho has an $L\alpha$ peak at 6.720 keV and an $M\alpha$ peak at 1.348 keV, and the $M\alpha$ peak is unlikely to be resolved from Al ($K\alpha$ 1.487 keV) in montmorillonite. Thus, it is assumed for this work that a small Ho peak at 6.720 keV in conjunction with Al and Si is diagnostic of the tracer. At this point, it should be noted that the tracer was not disaggregated following grinding and it is possible that some ‘clumping’ has occurred.

Figure 6 shows a typical example of an electron micrograph of a 50 T:50 M mixed floc. This shows individual microflocs of both dense, platy material typical of the tracer (to the left of the image) and flocs comprising biological and inorganic particles typical of those found in the natural estuarine mud (to the right of the image). EDS spectra collected from particles within these flocs confirm the identification of discrete microflocs of both tracer and natural mud. Particles in the microfloc to the left of the image are rich in Al, Si, Fe and Ho, suggesting that this aggregate predominantly comprised Ho-labelled montmorillonite. Particles in the microfloc to the right of the image are varied in composition. Particle A is rich in Ho, but not

Si or Al, and this may indicate the presence of a Ho precipitate, probably a hydroxide as REE precipitates are known to precipitate at $\text{pH} > 5$ (Bruque et al. 1980), rather than inclusion of tracer into the natural mud floc. Particle B is rich in Al, Si and Ho, suggesting that there has been some inclusion of tracer material into the floc, although this is not significant and is limited to the peripheral edge of the aggregate. Considerable analysis of these images failed to identify more Ho-rich particles. Thus, at the fine scale ($< 20 \mu\text{m}$), there has been little interaction between natural mud and the tracer with microflocs predominantly comprising either tracer or natural mud discretely.

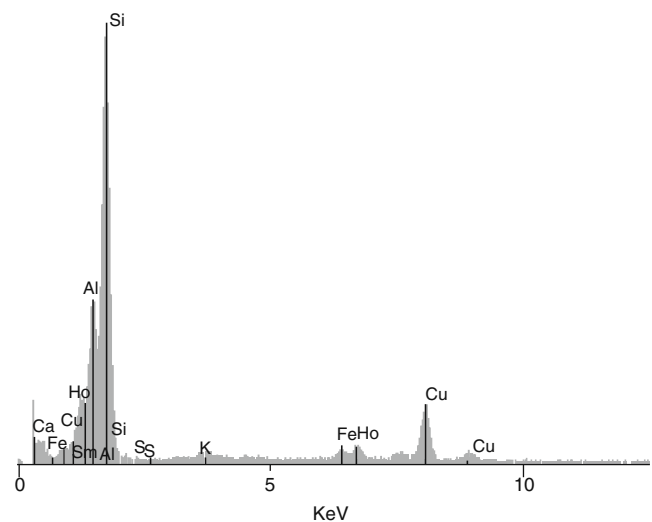
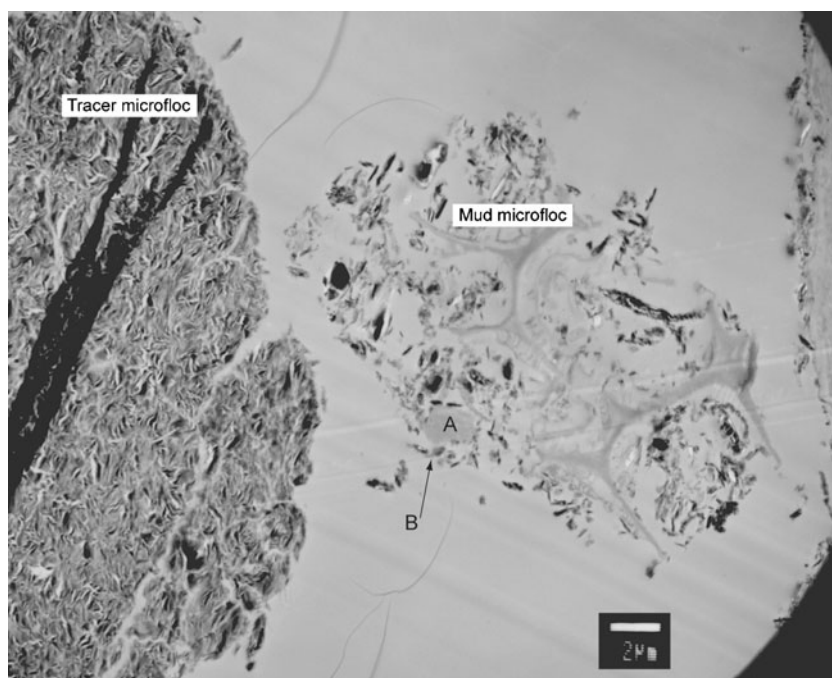


Fig. 5 EDS spectrum for a typical tracer floc

Fig. 6 Electron micrograph of mixed floc comprising 50% tracer and 50% natural mud (50 T:50 M)



4 Discussion

In order to satisfy the assumptions of tracer technology, a sediment tracer must have the same physical properties as the sediment that it is intended to mimic. For cohesive sediments, this means that the tracer must form flocs that have the same physical and dynamic properties as natural cohesive sediment and, therefore, must be incorporated into and transported via flocs (Black et al. 2007). The transport and fate of cohesive sediment in aquatic environments is largely controlled by its settling velocity and MSF, which are in turn controlled by particle size, shape, effective density and porosity (Williams et al. 2008). Consequently, these were the primary physical and dynamic characteristics observed for these experiments.

4.1 Physical characteristics of the tracer

The likelihood of particle collisions increases with turbulence and suspended sediment concentration, leading to aggregate growth (Winterwerp and van Kesteren 2004). However, as turbulence increases, the attractive forces holding flocs together will be overcome and flocs break apart. Therefore, floc size is also controlled by parameters which control floc stability such as the surface charge and roughness of colliding particles (Atkinson et al. 2005). Microbial secretions, such as EPS, increase the cohesiveness of muddy sediments (e.g. Paterson 1997) and are important for providing floc stability and strength due to bioflocculation (Droppo 2001), which can be clearly seen in the TEM images of the natural mud (Fig. 4a). Therefore,

in the absence of biological material, the tracer was expected to form weaker, smaller flocs, relying only on electrochemical flocculation for stability. Fractal dimensions were also calculated and are an indicator of floc compositional strength and stability (Kranenburg 1994). In marine systems, fractal dimension generally ranges from around 1.3 to 2.5, and a fractal dimension >2.2 is indicative of strong, compact estuarine flocs (Santschi et al. 2005; Winterwerp and van Kesteren 2004). Average fractal dimensions were >2.2 for total microfloc and macrofloc populations, suggesting that the tracer is capable of forming the stable macroflocs required for sediment deposition even without the presence of EPS.

As flocs increase in size, they have lower densities and higher porosity values as the flocs incorporate pore space, water and biological material into their structure (Droppo 2001, 2004). This can be observed for both the tracer and natural mud populations with porosity increasing and density decreasing with increasing floc size (Fig. 1). In addition, both the tracer and natural mud total floc populations show similar ranges for effective density and porosity values. Significant differences in effective density and porosity of the tracer and natural mud floc populations were not observed. However, the tracer formed the densest flocs (SB3, 418 kg m^{-3}) whilst the natural mud formed the least dense (SB7, 17 kg m^{-3}). Evidence of dense tracer microflocs (only microflocs $<20 \mu\text{m}$ could be observed) containing tightly packed minerogenic material can be seen in the TEM images (Fig. 4). These small microflocs are not large enough to have incorporated significant quantities of water and pore space into their structure, and as no

biological material was available in these experiments, they remain dense. In comparison, even the smallest natural mud microflocs contain biological material (Fig. 4). As the mean effective density of the tracer and natural mud microflocs are very similar, the tracer flocs must be incorporating large amounts of pore space as they aggregate compared to the natural mud. Although the calculated average porosity of the tracer and natural mud populations is similar, this is clearly evident for the smallest tracer microflocs (SB2) which have lower densities and higher porosities than the smallest natural mud flocs (SB3) and therefore must contain large amounts of pore space. However, the scale of the TEM images do not allow us to observe whole flocs $>20\ \mu\text{m}$ in diameter to confirm this. Therefore, the internal structure of the tracer and natural mud flocs must differ. The density variation across the range of floc sizes for both the tracer and natural mud populations is very small, and the effective density, particularly of the macroflocs, is very close to that of water. Therefore, the differences observed are unlikely to influence settling velocity greatly (Droppo 2001, 2004).

Particle shape also affects the settling potential of flocs due to resistance against the carrying medium (Li and Ganczarczyk 1987), and consequently, sediment transport models will often use a characteristic floc shape, or fractal mathematics, to account for the influence of shape on floc behaviour (Kranenburg 1994; Lee et al. 2000; Williams et al. 2008; Winterwerp 1998). The presence of organic matter typically results in elongate “stringer” natural mud flocs (Chen et al. 2005) as observed here, whilst the tracer flocs, which contain no organic matter, are more spheroidal in shape. It is possible that shape may result in differing dynamic behaviour for the tracer flocs; however, shape is generally considered to be less important than other factors such as diameter for controlling settling velocity (e.g. Williams et al. 2008).

4.2 Dynamic characteristics of the tracer

Settling velocity is one of the key dynamic input parameters required for sediment transport models and is dependent primarily upon particle size (Droppo 2004; Fennessy et al. 1994), although porosity, fractal dimension and particle shape may also be important (Santschi et al. 2005; Williams et al. 2008). As macroflocs account for the majority of MSF in the estuarine environment, it is fundamental that a cohesive sediment tracer should exhibit similar dynamic behaviour to natural sediment, in particular for the macrofloc population. Settling velocities for both tracer and natural mud floc populations are within the same range, and although the tracer microflocs settle more slowly than the natural mud, there are no statistical differences between the macrofloc populations. Slower settling velocities for the

microflocs are primarily due to their smaller particle size, and although the tracer microflocs are more spheroidal in shape with higher porosities, this does not significantly increase their settling velocities.

Distribution of SPM and mass settling flux over the floc size spectrum are also important parameters for understanding settling behaviour, and both show very different patterns for the tracer and natural mud. Here, although mass is clearly distributed differently for both the tracer and natural mud, average settling velocities for the macroflocs can not be distinguished statistically. This highlights the importance of measuring settling velocity rather than estimating velocity from particle size data.

4.3 Interaction of the tracer and natural mud

The interaction of the tracer and natural mud at both fine and gross scales has been examined by observing the physical and dynamic floc characteristics of tracer and natural mud mixtures. The pure tracer and natural mud form statistically different microfloc populations in terms of D . As tracer content increases from 25% to 100%, there is an overall decrease in floc size and the flocs formed are more spheroidal in shape (Fig. 2). This suggests that organic matter is important for maintaining both microfloc structural stability and shape and suggests that the tracer and mud are interacting. However, individual microflocs (only microflocs $<20\ \mu\text{m}$ can be observed) containing both tracer and natural mud were not observed, suggesting that primary particles of tracer and natural mud do not interact and flocculate. Rather, microflocs comprising either tracer or natural mud interact to form larger mixed flocs where the tracer can be identified as discrete, densely packed microflocs within the gross floc structure. This order of aggregation agrees with the early research of Krone (1962) and later work by Eisma (1986).

Macroflocs comprising tracer and natural mud mixtures are larger and settle faster than either the pure tracer or pure natural mud macroflocs. We hypothesise that this is due to irregular packing of the differently shaped natural mud (stringer) and tracer (spheroidal) flocs. This again supports the order of aggregation observed in the microflocs with the presence of tracer significantly changing the resultant floc shape. Therefore, the addition of even a small amount of tracer to the natural muddy material appears to change the structure of the flocs formed. Unfortunately, the scale of the TEM analysis does not allow us to examine the internal structure of the macroflocs in more detail.

4.4 Conclusions and potential application of cohesive sediment tracers for understanding sediment transport

The Ho-labelled montmorillonite tracer developed here clearly flocculates. The tracer microflocs, which are

considered to be the building blocks for larger aggregates, are smaller and settle more slowly than natural mud. However, the tracer macroflocs, which are fundamental to sediment transport, have key physical and dynamic characteristics which cannot be distinguished from the natural cohesive mud used in these experiments. However, the tracer forms macroflocs that are sub-spheroidal in shape with greater pore space compared to the elongate “stringer” natural mud flocs. At both fine and gross scales, there is evidence to suggest that the tracer and natural mud interact. However, this interaction is not on a primary particle-to-particle basis; rather, macroflocs comprised discrete microflocs of pure tracer or pure natural mud. Therefore, the tracer meets the fundamental requirements of tracer technology.

Because of the differences in natural mud and tracer floc shape, the mixed macroflocs (T/M) are more irregularly packed, resulting in a larger size, lower effective density and slightly increased porosity compared to end member flocs. This is most evident for the mixed floc comprising 25% tracer which also has the highest settling velocity and mass settling flux, suggesting that when tracers and natural sediment interact in the natural environment, their dynamic transport characteristics may differ from natural muddy material.

The suspended sediment concentrations used and the levels of turbulence applied are known to stimulate flocculation and be representative of estuarine waters. However, the manner in which the tracer and natural mud were introduced in these experiments is unlikely to represent natural sediment mixing in the water column, and this may have influenced the interaction of the two materials. There are no adopted protocols for the deployment of cohesive tracers in the literature and methods of tracer release vary. Generally, tracers are placed on the seabed and once entrained interact with natural material in suspension (Black et al. 2007). Cohesive tracers have also been introduced to natural muddy material within the supply line of dredgers before being released to coastal waters (e.g. Louise et al. 1986). To our knowledge, no investigations have examined how the introduction of a cohesive tracer to the environment may influence its interaction with natural material, and this requires further investigation.

Following deployment, a sediment tracer will undergo many orders of magnitude of dilution in the environment. Therefore, in order to understand better the interaction of cohesive sediment tracers and natural muddy material in realistic environmental settings, there is a need to examine floc interaction and structure both in laboratory experiments under a wider range of tracer to natural mud ratios and in situ. For example, it may take a few minutes to several days for flocs to equilibrate with in situ hydrodynamic con-

ditions (Winterwerp and van Kesteren 2004); therefore, it is possible that under these experimental conditions, the tracer and natural mud flocs had not fully equilibrated. We may also need to consider further the influence of tracer mineralogy. Here, we have used montmorillonite which flocculates faster but produces smaller floc sizes than for example illite which is perhaps a more common mineral in many estuarine environments. Therefore, the results of this work have implications for the mechanisms by which tracers are deployed in the estuarine environment.

In terms of matching the physical and dynamic characteristics of natural mud, this cohesive sediment tracer is superior to commercially available, synthetic tracer particles which are hydrophobic and only match natural sediment in terms of size and shape. However, even here, the dynamic characteristics (size, settling velocity and MSF) of mixed tracer and natural mud flocs differ significantly from natural muddy material. Therefore, if cohesive sediment tracers, and synthetic tracers in particular, continue to be used to infer sediment transport pathways and inform sediment transport models, their interaction with natural muddy material and their dynamic behaviour in natural environments need to be fully understood.

Acknowledgements Analytical work for this project was funded by NERC (NER/D/S/2003/00706) and the Leverhulme Trust (RF/4/2006/0114). Travel expenses for K. Spencer to the NWRI in Canada were funded by the Foundation for Canadian Studies in the United Kingdom. Expert assistance with electron spectro-microscopy was provided by M.M. Reid.

References

- Adams EE (1998) Deposition of contaminated sediments in Boston Harbor studied using fluorescent dye and particle tracers. *Estuar Coast Shelf Sci* 46(3):371–382
- Atkinson JF, Chakraborti RK, Van Benschoten JE (2005) Effects of floc size and shape in aggregation. In: Droppo IG, Leppard GG, Liss SN, Milligan TG (eds) *Flocculation in natural and engineered systems*. CRC, Boca Raton, p 438
- Benson T, French JR (2007) InSiPID: a new low-cost instrument for in situ particle size measurements in estuarine and coastal waters. *J Sea Res* 58:167–188
- Black KS, Athey S, Wilson P, Evans D (2007) The use of particle tracking in sediment transport studies: a review. *Special Publications*, vol 274, Geological Society, London, pp 73–91
- Bouyer D, Coufort C, Line A, Do-Quang (2005) Experimental analysis of floc size distributions in a 1-L jar under different hydrodynamics and physico-chemical conditions. *J Colloid Interface Sci* 292:413–428
- Bruque S, Mozas T, Rodriguez A (1980) Factors influencing retention of lanthanide ions by montmorillonite. *Clay Miner* 15:413–420
- Buffle J, Leppard GG (1995) Characterization of aquatic colloids and macromolecules. 2. Key role of physical structures on analytical results. *Env Sci Tech* 29:2176–2184
- Chen MS, Wartel S, Temmerman S (2005) Seasonal variations of floc characteristics on tidal flats, the Scheldt Estuary. *Hydrobiologia* 540:181–195

- Courtois G, Monaco A (1969) Radioactive methods for the quantitative determination of coastal drift rate. *Mar Geol* 7:183–206
- Droppo IG (2001) Rethinking what constitutes suspended sediment. *Hydrol Proc* 15(9):1551–1564
- Droppo IG (2004) Structural controls on floc strength and transport. *Can J Civ Eng* 31:569–578
- Droste RL (1996) Theory and practice of water and wastewater treatment. Wiley, London
- Dyer KR, Bale AJ, Christie MC, Feates N, Jones S, Manning AJ (2002) The turbidity maximum in a mesotidal estuary, the Tamar Estuary, UK. Part II: the floc properties. In: Winterwerp JC, Kranenburg C (eds) *Fine sediment dynamics in the marine environment—Proc Mar Sci 5*. Elsevier, Amsterdam
- Eisma D (1986) Flocculation and de-flocculation of suspended matter in estuaries. *Neth J Sea Res* 20(2/3):183–199
- Environmental Protection Agency (1999) Enhanced coagulation and enhanced precipitative softening guidance manual. United States Environmental Protection Agency, Office of Water, Report no. EPA 815-R-99-012
- Fennessy MJ, Dyer KR, Huntley DA (1994) Size and settling velocity distributions of flocs in the Tamar Estuary during a tidal cycle. *Neth J Aquat Ecol* 28:275–282
- Field A (2009) *Discovering statistics using SPSS*, 3rd edn. Sage, London
- Gerba CP, McLeod JS (1976) Effect of sediments on the survival of *Escherichia coli* in marine waters. *Appl Environ Microbiol* 32:114–120
- Grapentine L, Webber J, Thompson S, Milani D, Labelle H, Droppo I, Spencer KL (2007) Toxicity of holmium-labelled clay of four benthic invertebrates. National Water Research Institute, Technical Report WSTD Contribution no. 07-541
- Heathershaw AD, Carr AP (1978) Measurement of sediment transport rates using radioactive tracers. In: *Coastal Sediments '77* (ASCE Symposium, Charleston, South Carolina 1977). American Society of Civil Engineers, New York, pp 399–416
- Hudson HE (1981) *Water clarification processes: practical design and evaluation*. Van Nostrand Reinhold, Environmental Engineering Series
- Kranenburg C (1994) The fractal structure of cohesive sediment aggregates. *Est Coast Shelf Sci* 39:451–460
- Krezoski JR (1985) Particle reworking in Lake Michigan sediments: in-situ tracer measurements using a rare earth element. 28th Conf Great Lakes Res, International Association of Great Lakes Research, Milwaukee, WI
- Krone RB (1962) Flume studies of the transport of sediment in estuarial shoaling processes. Final report hydraulic engineering laboratory and sanitary engineering research laboratory. University of California at Berkeley, Berkeley, CA
- Le Roux JP, Rojas EM (2007) Sediment transport patterns determined from grain size parameters: overview and state of the art. *Sed Geol* 202:473–488
- Lee DG, Bonner JS, Garton LS, Ernest ANS, Autenrieth RL (2000) Modeling coagulation kinetics incorporating fractal theories: a fractal rectilinear approach. *Wat Res* 34:1987–2000
- Li DH, Ganczarzyk J (1987) Stroboscopic determination of settling velocity, size and porosity of activated sludge flocs. *Wat Res* 21:257–262
- Liss SN, Droppo IG, Flannigan DT, Leppard GG (1996) Floc architecture in wastewater and natural riverine systems. *Env Sci Tech* 30:680–686
- Louisse CJ, Akkerman RJ, Suylen JM (1986) A fluorescent tracer for cohesive sediment. International Conference on Measuring Techniques of Hydraulics Phenomena in Offshore, Coastal and Inland Waters. London, England, 9–11 April 1986, pp 367–391
- Mahler BJ, Bennett PC, Hillis DM, Winkler M (1998a) DNA-labeled clay: a sensitive new method for tracing particle transport. *Geol* 26:831–834
- Mahler BJ, Bennett PC, Zimmerman M (1998b) Lanthanide-labelled clay: a new method for tracing sediment transport in karst. *Ground Wat* 36:835–843
- Manning AJ (2001) A study of the effects of turbulence on the properties of flocculated mud. PhD thesis, Institute of Marine Studies, University of Plymouth
- Manning AJ (2004a) The observed effects of turbulence on estuarine flocculation. In: Ciavola P, Collins MB (eds) *Sediment transport in European estuaries*. *J Coast Res SI* 41:90–104
- Manning AJ (2004b) Observations of the properties of flocculated cohesive sediment in three western European estuaries. *J Coastal Res SI* 41:70–81
- Manning AJ (2006) LabSFLOC—a laboratory system to determine the spectral characteristics of flocculating cohesive sediments. HR Wallingford Technical Report, TR 156
- Manning AJ, Dyer KR (2002) The use of optics for the in-situ determination of flocculated mud characteristics. *J. Optics A: Pure and Applied Optics*, Institute of Physics Publishing, 4, pp S71–S81
- Manning AJ, Dyer KR (2007) Mass settling flux of fine sediments in Northern European estuaries: measurements and predictions. *Mar Geol* 245:107–122
- Manning AJ, Friend PL, Prowse N, Amos CL (2007) Preliminary findings from a study of Medway Estuary (UK) natural mud floc properties using a laboratory mini-flume and the LabSFLOC system. *Cont Shelf Res BIOFLOW SI*, pp 1080–1095
- McLaren P, Bowles D (1985) The effects of sediment transport of grain-size distributions. *J Sed Pet* 55:457–470
- McLaren P, Hill SH, Bowles D (2007) Deriving transport pathways in a sediment trend analysis (STA). *Sed Geol* 202:489–498
- Mietta F, Chassagne C, Manning AJ, Winterwerp JC (2009) Influence of the physico-chemical properties of the suspension on turbulence-induced mud flocculation. *Ocean Dynamics, Physics of Estuaries & Coastal Seas*, PECS-2008 Special Issue
- Newmann KA, Morel FMM, Stolzenbach KD (1990) Settling and coagulation characteristics of fluorescent particles determined by flow-cytometry and fluorometry. *Env Sci Tech* 24:506–513
- Paterson DM (1997) Biological mediation of sediment erodibility: ecology and physical dynamics. In: Burt N, Parker R, Watts J (eds) *Cohesive sediments*. Wiley, Chichester, pp 215–229
- Poizot E, Mear Y, Biscara L (2008) Sediment trend analysis through the variation of granulometric parameters: a review of theories and applications. *Earth Sci Rev* 86:15–41
- Santschi PH, Burd AB, Gaillard J, Lazarides AA (2005) Transport of materials and chemicals by nanoscale colloids and micro- to macro-scale flocs in marine, freshwater and engineered systems. In: Droppo IG, Leppard GG, Liss SN, Milligan TG (eds) *Flocculation in natural and engineered systems*. CRC, Boca Raton, p 438
- Silva A, Taborda R, Rodrigues A, Duarte J, Cascalho J (2007) Longshore drift estimation using fluorescent tracers: new insights from an experiment at Comporta Beach, Portugal. *Mar Geol* 240:137–150
- Spencer KL, Suzuki K, Benson T, Taylor JA, Manning A, Dearnaley M (2007) The potential use of geochemically labelled minerals as tracers for cohesive sediments. In: Westrich B, Förstner U (eds) *Sediment dynamics and pollutant mobility in rivers—interdisciplinary approach*. Springer, Berlin
- ten Brinke WBM (1993) The impact of biological factors on the deposition of fine grained sediment in the Oosterschelde (the Netherlands). PhD thesis, University of Utrecht
- Tonk A, Masselink G (2007) Evaluation of longshore transport equations with OBS sensors, streamer traps, and fluorescent tracer. *J Coast Res* 21:915–931

- van Leussen W (1994) Estuarine macroflocs and their role in fine-grained sediment transport. PhD thesis, University of Utrecht
- Williams ND, Walling DE, Leeks GJL (2008) An analysis of the factors contributing to the settling potential of fine fluvial sediment. *Hydrol Proc* 22:4153–4162
- Winterwerp JC (1998) A simple model for turbulence induced flocculation of cohesive sediment. *J Hydr Res* 36:309–326
- Winterwerp JC, van Kesteren WGM (2004) Introduction to the physics of cohesive sediment in the marine environment. In: van Loon T (ed) *Developments in sedimentology*, 56. Elsevier, Amsterdam
- Yin Y, Chang N, Zhong W, Sun S, Zhang Y, Cui H, Chen S, Feng Y, Sun L (1993) A study of neutron activation tracer sediment technique. *Sci China Ser A* 36:243–248